

MuSCAT3 Release Notes

Daniel Harbeck, Nikolaus Volgenau, Norio Narita, Akihiko Fukui, Mark Bowman, Mark Elphick, JD Armstrong, Jacqueline Han, Jon Nation, Elisabeth Heinrich-Josties, Steve Foale, Matt Daily, Curtis McCully, Annie Kirby, Cary Smith, Brian Haworth, Lisa Storrie-Lombardi, Patrick Conway, Joey Chatelain, Etienne Bachelet, Marshall Johnson, Markus Rabus, Fernando Rios, Sarah Rettinger, Wayne Rosing

Updated April 19th, 2021

This document outlines the performance of the MuSCAT3 instrument at the time of its first release and after subsequent updates. The information herein will allow new MuSCAT3 users to ramp up their science programs. MuSCAT3 users should diligently evaluate their data and adjust the setup of their observations accordingly.

MuSCAT3 is not only a new instrument, but as a multi-channel imager it is also a new *type* of instrument at LCO. The LCO operations team will learn how to maintain MuSCAT3 as the LCO user community learns how to use it. Users should provide feedback or ask questions via science-support@lco.global.

Overall, MuSCAT3 is performing well. However, full characterisation is not complete, and there remain a few loose ends that will be addressed over the next couple of months. (See the Limitations section below.) Some operational interruptions may be necessary when we make improvements.

What's New?

Since the release notes 1.2 from Feb 1 2021:

1. The zs band camera was exchanged. The Sophia 2048 BX camera is installed, as in the original design, and the Pixis camera is decommissioned. The sensitivity in the zs band is improved, and the fringe pattern amplitude is suppressed. These effects increase the overall S/N in the zs channel.
2. The photonic diffuser mechanisms have been partially repaired. Observations with the diffusers, albeit with limitations, are now possible.

Data Processing & Format

MuSCAT3 images are processed by the BANZAI pipeline. Standard CCD calibrations such as bias, dark, and sky flat fields are acquired by the observatory for use in BANZAI processing. Calibrations are available in the science archive. Flat fields in the two readout modes (see below) are acquired during morning and evening twilight on alternating nights.

Images from each of MuSCAT3's four channels are stored in individual FITS files. Image names follow the typical LCO name convention, e.g. `ogg2m001-ep02-20201023-0157-e91.fits.fz`. The camera codes for the four MuSCAT3 channels are:

g': ep04
 r': ep02
 i': ep03
 zs: ep05.

For data taken before March 1, 2021, the zs band camera is ep01.

The image numbers increment independently for each channel. Users should not expect the first image (in a series of exposures) from each channel to have identical image numbers.

Detector performance

MuSCAT3 supports FAST and SLOW CCD readout modes. The readout overheads are <6 seconds and 46 seconds, respectively. The CCD readout mode is set for all four channels simultaneously. The read noise and full well of the cameras in the different readout modes are given in the table below:

| Passband | Read Noise [e-] FAST / SLOW mode | Full well [ke-] | Gain [e-/ADU] |
|----------|-------------------------------------|-----------------|------------------|
| g' | 12 / 3.5 | 120 | 1.9 |
| r' | 12 / 3.5 | 120 | 1.88 |
| i' | 12 / 3.5 | 82 | 1.8 |
| zs ep01 | 15 / 3.5 | 71 | 1.7 |
| zs ep05 | ~15 / 5 | >100 | 2.0 ¹ |

The g',r',i' cameras read at 100kHz and 2 MHz pixel rates in the SLOW and FAST mode, respectively. The Sophia camera intrinsically offers three speed modes: 100kHz, 1 MHz, and 4 MHz with readout times of <3, 6, and 45 seconds, respectively. We have elected to map the slow and fast modes for the zs-band to 1 MHz and 4MHz, respectively. Based on user feedback, this decision can be subject to a future review.

The Sophia camera (zs band) 4 MHz readout has the benefit of a very short readout overhead (order of 2.5 seconds). The downside is the generation of spurious charge, which is visible as a

¹ The gain measurement of ep05 varies between 1.7e- and 2.1e-, which we attribute to the spurious charge. A refined measurement is in preparation.

ramp in the background level of a bias readout. The spurious charge is corrected by a bias subtraction but contributes of the order of 5 electrons RMS to the read noise budget.

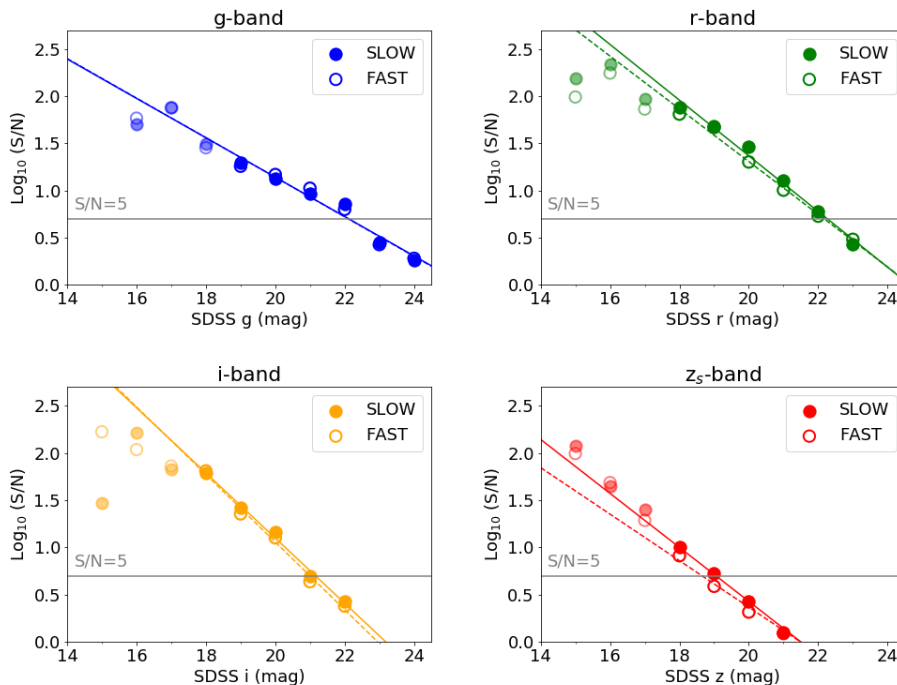
Photometric Performance

The *photometric zero points* of MuSCAT3 were estimated from science validation observations.

The *limiting (S/N=5) magnitudes* were measured during first light (Pixis camera in zs band) at airmass 1.3 for a 10 minute exposure in the SLOW / FAST readout mode respectively: g': 22.1 / 22.1 mag; r': 22.3 / 22.2 mag; i': 21.2 / 21.0 mag; z': 19.1 / 18.7 mag. These results are shown in the figures below. The limiting magnitudes in both readout modes with the new Sophia camera in the zs bands were measured in March 2021 at 20.2 / 20.2 mag, i.e., an improvement on the order of 1 magnitude.

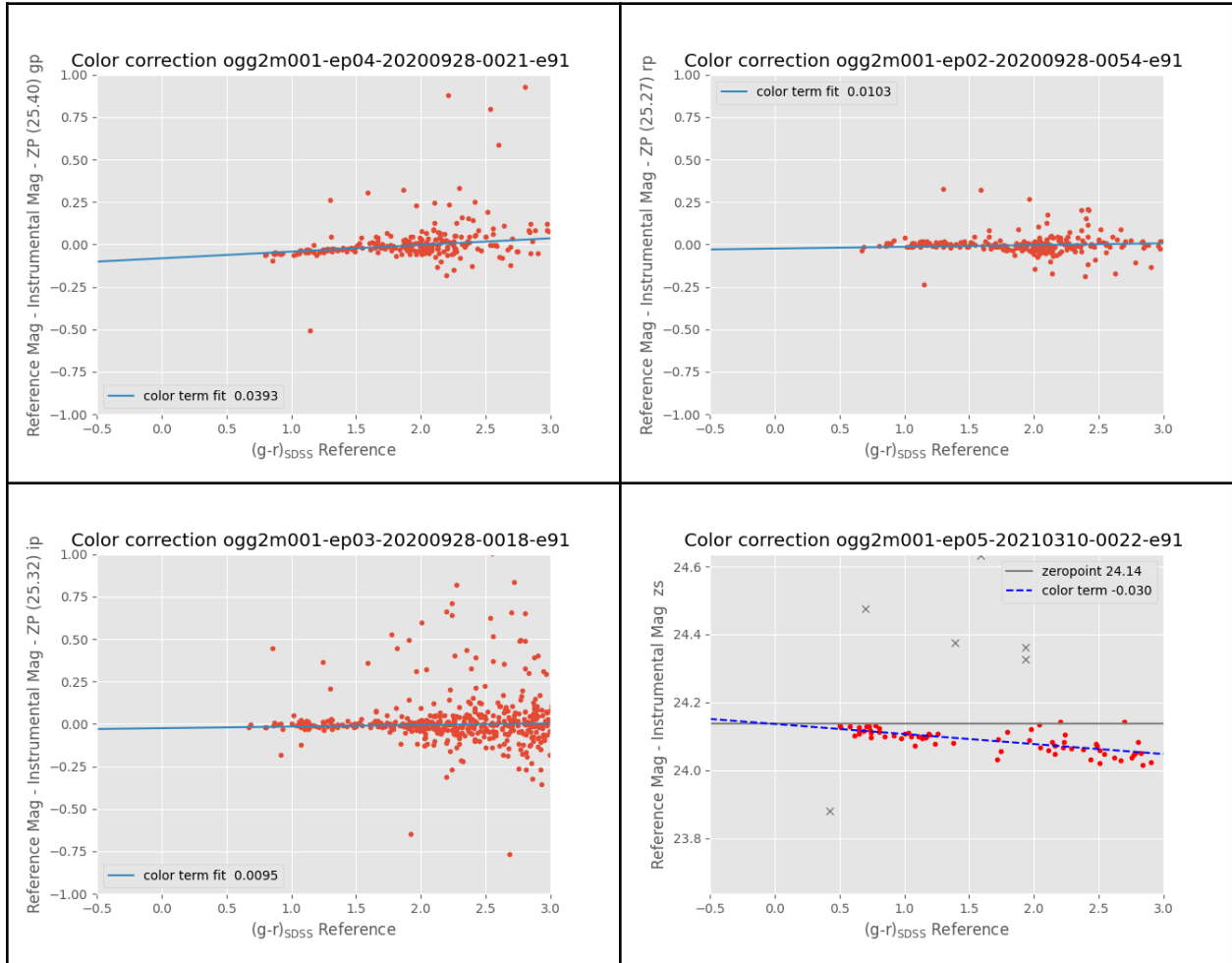
In this final configuration, the *photometric zeropoints* changed in comparison to the previously installed Spectral camera by: g': +0.5 mag; r': +0.1 mag; i': -0.15 mag; z': +0.8 mag.

These limiting magnitudes differ from the results produced by the LCO exposure time calculator, and users are advised to independently verify that their data meet their expectations. The calculator is being updated; it currently assumes 100% transparency.



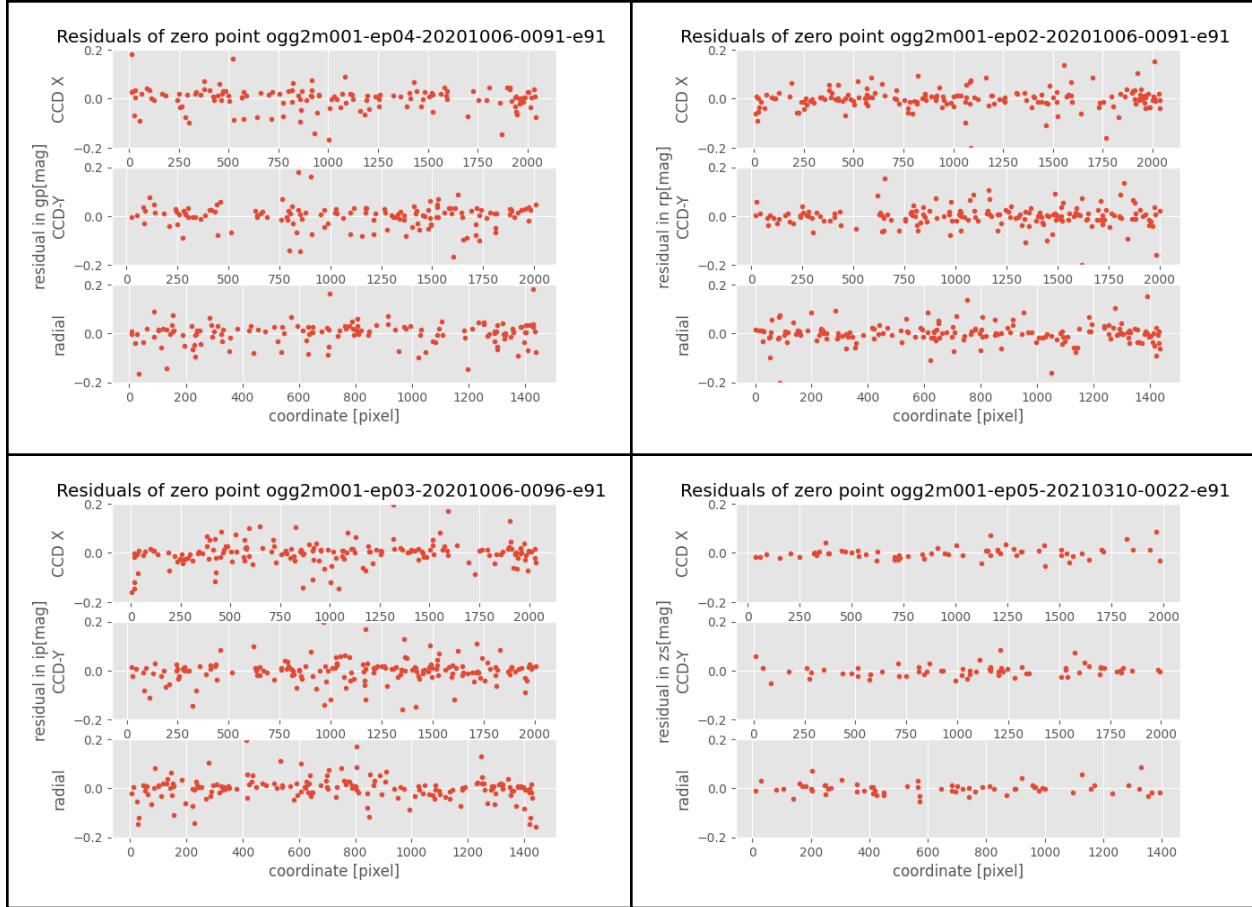
Color terms

The instrumental *color terms* are represented in the figure below as a correction versus the SDSS reference color in $g'-r'$. Users should expect to color-correct photometry at least in the g' and z_s bands according to their program's needs.



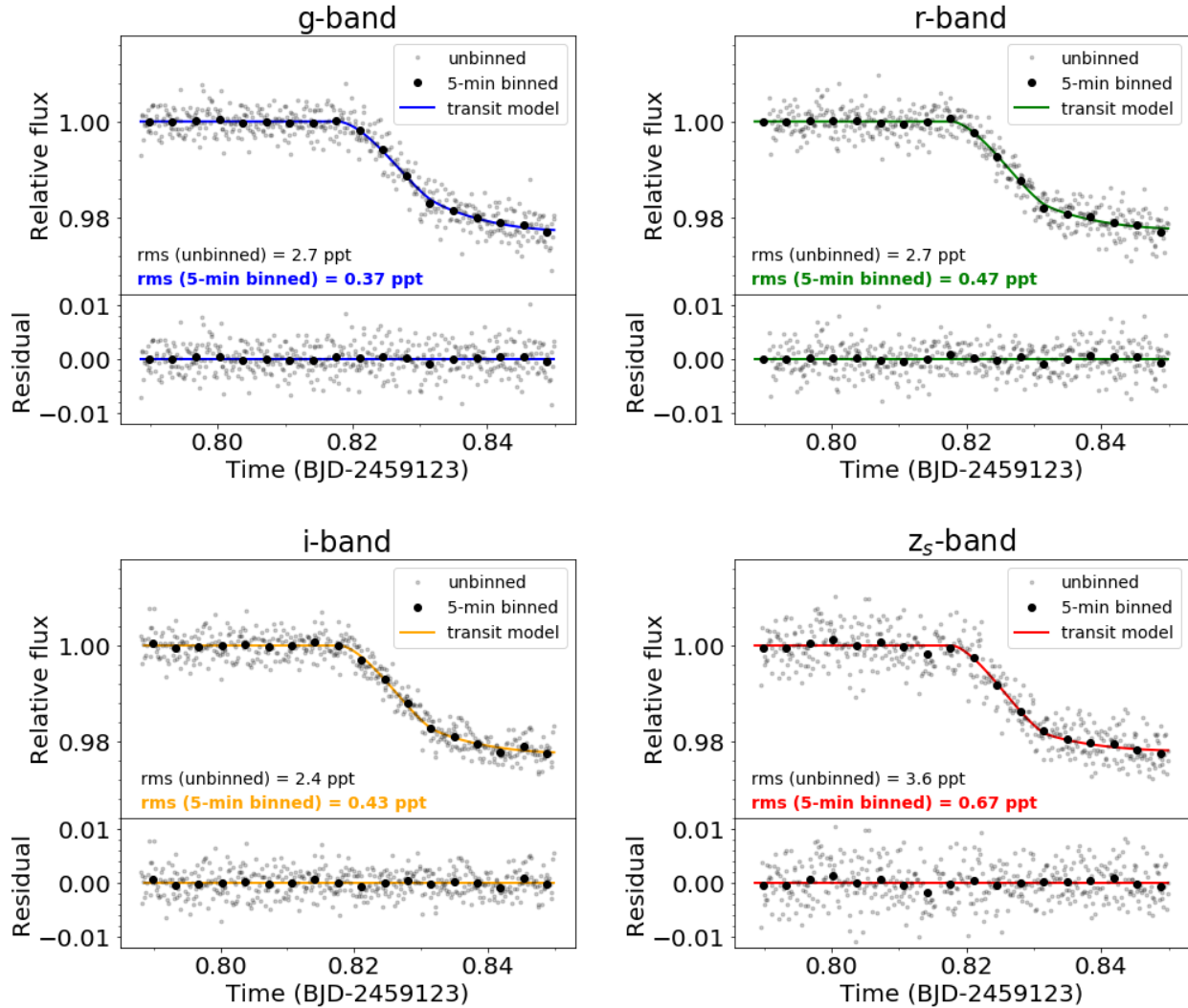
Homogeneity over the field of view

There is currently no evidence of significant photometric zeropoint shifts over the field of view. The following graphs exemplify the residual of the color corrected zeropoint plotted as a function of the x , y coordinates, as well as the radial distance from the detector center. Independent analysis of other observations yielded similar results on homogeneity.



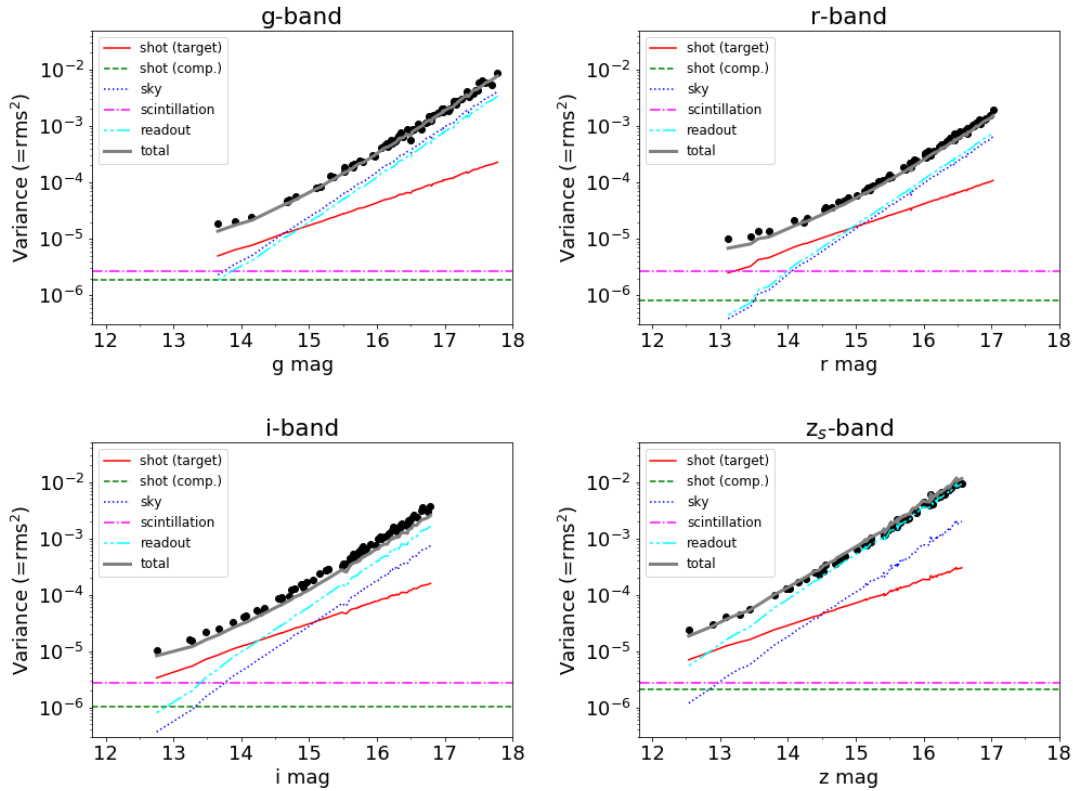
Demonstration of time series photometry

One of the key motivations of MuSCAT3 is observing time-variable objects, such as transiting planetary systems, for several hours within one night. To demonstrate the achievable photometric precision with MuSCAT3, we observed a transit of Qatar-1b, a known Jovian-sized planet orbiting a K dwarf with magnitudes of $g=13.4$, $r=12.7$, $i=12.3$, and $z=12.1$, on October 1, 2020 UT. The target field was observed with exposure times of 5 seconds and the FAST readout mode for all bands. The focus offset was +2 mm. Only the transit ingress was observed for technical reasons. Telescope guiding was not operational during the observation (see Limitations section), resulting in significant displacements of stellar positions on the detectors over the 90-minute-long observation (by ~ 30 pixels in both X and Y directions due to the telescope tracking drifts).



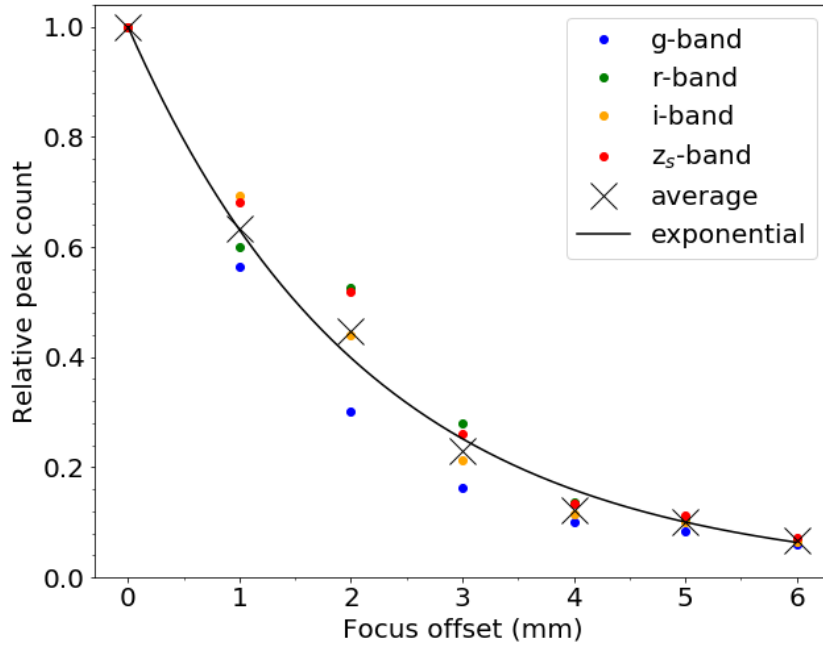
The above light curves were produced by aperture photometry with an aperture size of 12 pixels (3.2 arcsec). Several comparison stars with similar brightness to the target star were used for the relative photometry. The achieved photometric precisions, i.e., rms of the residuals from a transit-model fit, were 2.7, 2.7, 2.4, and 3.6 ppt per exposure, and 0.37, 0.47, 0.43, and 0.67 ppt per 5 minutes, for g, r, i, and z_s bands, respectively.

We also measured the photometric precisions (rms) of dozens of non-variable stars in the same field as Qatar-1. A single non-variable star with a similar brightness to Qatar-1 was used as a comparison star. As shown in the following figure, the measured light-curve dispersions can be explained by the sum of the known errors, i.e., shot noises of the target and comparison stars, sky background noise, readout noise, and scintillation noise. This result demonstrates that the contributions from systematic (unknown) noises are negligible, even without guiding, at least for the magnitude range demonstrated here.



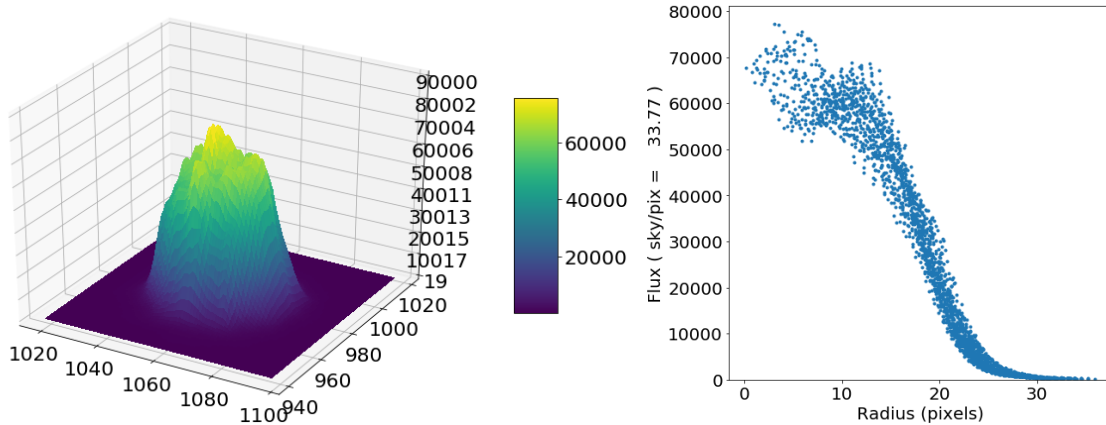
Relation between focus value and peak count

MuSCAT users may want to defocus to avoid saturation and/or to achieve higher photometric precision for bright targets. The relation between the focus offset and the stellar peak count was investigated by imaging targets at airmass=1.1 on a night when the natural seeing was $\sim 0.8''$, as shown in the plot below. Note that the data for 0 offset could not be obtained under the same sky conditions, and the peak count for 0 offset was estimated using a Moffat function with FWHM of $0.8''$. The peak count decays roughly as an exponential function with $\exp(-0.46 \times [\text{focus (mm)}])$. You can find more information about the relation between focus value and peak count from Akihiko Fukui's [MuSCAT3 peak count estimator](#).

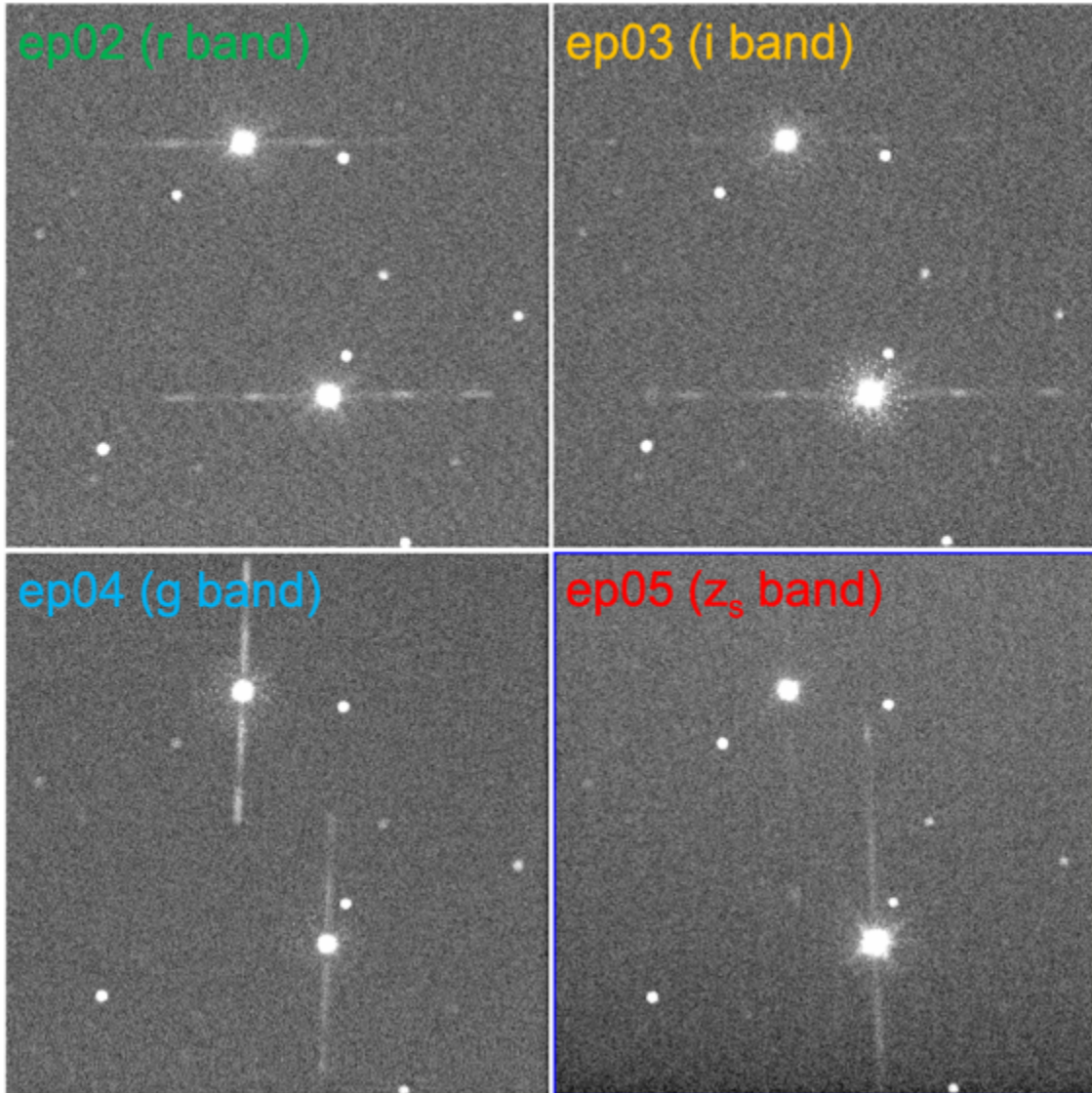


Photonic Diffusers

MuSCAT3 is equipped with photonic diffusers manufactured by RPC Photonics Inc. (Engineered Diffusers™ with an opening angle of 0.34 deg) that can be moved into the beam via a linear stage. The diffusers provide an alternative to defocusing the telescope to prevent bright target saturation. The diffusers expand the point spread function to an 11" diameter top-hat profile. The figure below shows radial profiles (right) of 55 Cnc observed for 2 seconds through the gp band with the diffuser IN the optical path.



Note that the diffusers create their own large-scale patterns:



The streak patterns extend in the vertical or horizontal direction, depending on the channel, with a length of ~ 1500 pixels. In the streaks, the counts per pixel are at most $\sim 2 \times 10^{-4}$ of the peak counts of the star.

A diffuser's position can be controlled via API calls or the web portal for each of the four Muscat channels. The positions are called IN and OUT (of the beam). The IN / OUT position is indicated by the FILTER keyword in the FITS header. If a diffuser is out, the FILTER keyword will be the passband's filter, e.g., gp. If the diffuser is in the beam, the FILTER keywords will be e.g. gp*diffuser.

Flat fields with the diffuser in the IN and OUT position differ in their fine structure, and sky flats are acquired with diffusers both IN and OUT.

The use of photonic diffusers is offered as a shared risk option. Users are advised to take their own test data before requesting long observations.

Telescope Guiding

Telescope guiding can be achieved in two ways, selectable by the user at the time of observation submission.

1. *Using the facility guider.* This guide mode allows telescope guiding even if MuSCAT3 exposure times are long compared to the time scale of telescope tracking errors (>30 seconds). However, because the facility guide camera has a lower sensitivity and a small field-of-view (4'x3'), guide stars are not available everywhere on sky.
2. *Using MuSCAT3 images to self-guide.* Although the MuSCAT3 field-of-view (9'x9') will usually contain enough guide stars, self-guiding is beneficial only if images are acquired on a time scale faster than the tracking errors, i.e, with exposure times < 30 seconds. If MuSCAT3 readouts are > 30 seconds apart, guiding performance will decline. *Initial testing indicates that Muscat self-guiding can work with the diffusers in the beam.* In general, self-guiding will be most useful for observations with the following configuration:
 - a. Type = Exposure Sequence (In the API language: type = REPEAT_EXPOSE)
 - b. Exposure Mode = Asynchronous
 - c. $2 \text{ s} < \text{Exposure Time} < 30 \text{ seconds}$ (in at least one channel)

If Guiding is set to On, then guiding will be attempted using the facility guider. If the attempt fails, the observation will be discontinued. If Guiding is set to Optional, then guiding will also be attempted with the facility guider, but if the attempt fails, the observation will continue without guiding. If Guiding is set to Off, then self-guiding will be used. The channel chosen for guiding will be the one with the shortest exposure time that is greater than 5 seconds.

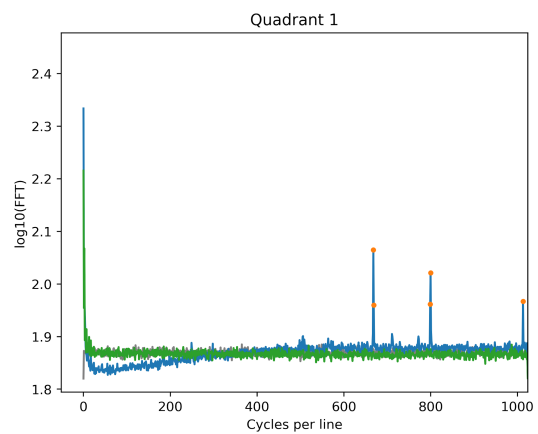
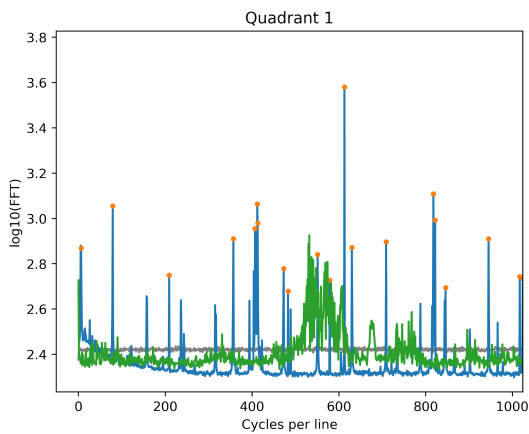
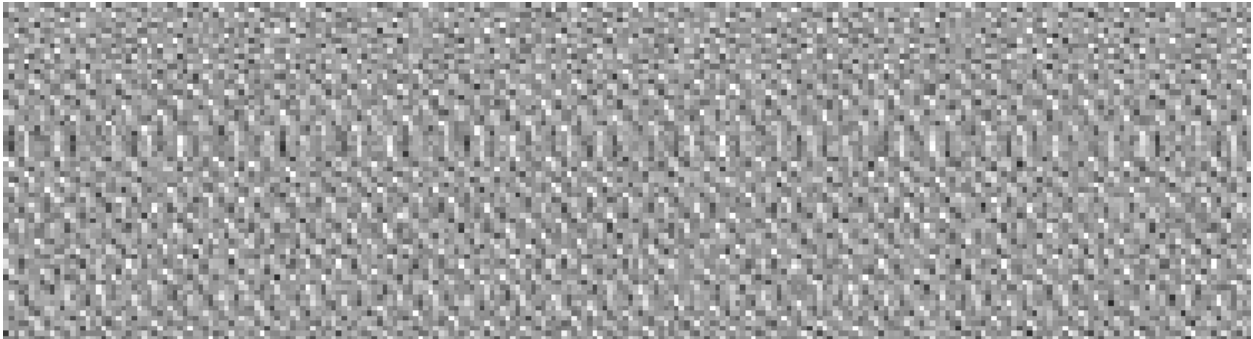
The section on telescope tracking (below) describes the importance of guiding during MuSCAT3 observations. **Observers are strongly advised to verify, e.g. with a short test before their science observation, that their selected guide strategy meets their needs. This advice particularly applies to time-critical observations such as exoplanet transits.**

Known Limitations

Pattern noise

All Princeton Instruments Pixis cameras (g'r'i') show elevated pattern noise when the FAST readout mode is used. The source of noise is under investigation, but it may be an inherent

feature of the Pixis camera fast readout mode. No such pattern noise is observed in any readout mode of the Sophia (zs) camera.



Top: Pattern noise is visible in this zoom-in into a bias frame, acquired in the FAST readout mode. The power spectrum (blue: x-direction, green: y-direction) of a bias (ep02) taken in the FAST readout mode (lower left) illustrates the pattern noise. The power spectrum of the SLOW readout mode (lower right) is very clean. The read noise is 12 and 3.5 electrons, respectively, but note that in the FAST readout more, the noise is non-gaussian.

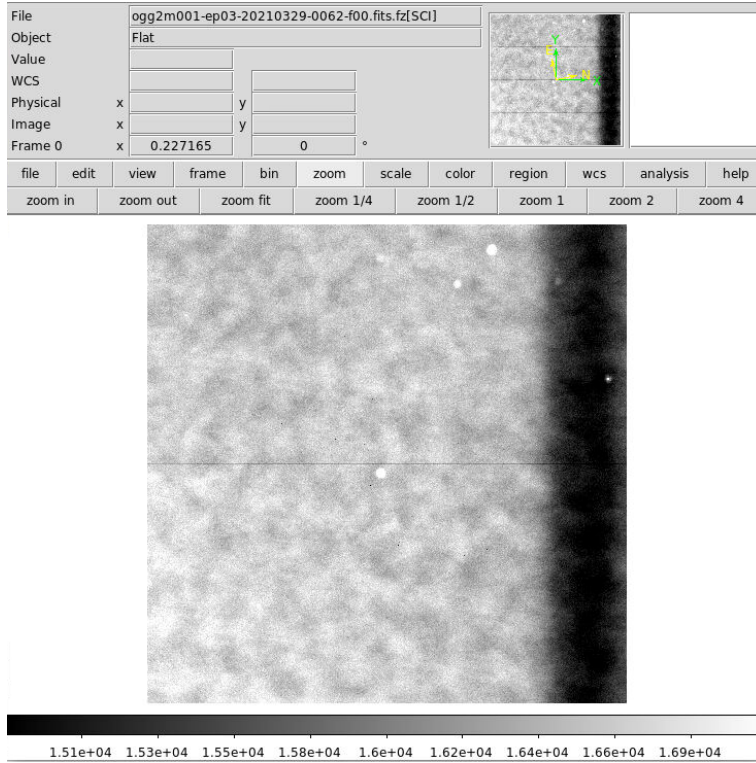
Shutter imprint

The Pixis and Sophia cameras both utilize an iris-type shutter. The opening and closing motion of the shutter can leave an illumination imprint on images. The example below shows a flat field exposure with 0 seconds exposure time (i.e. open and immediate close action) to illustrate the imprint.



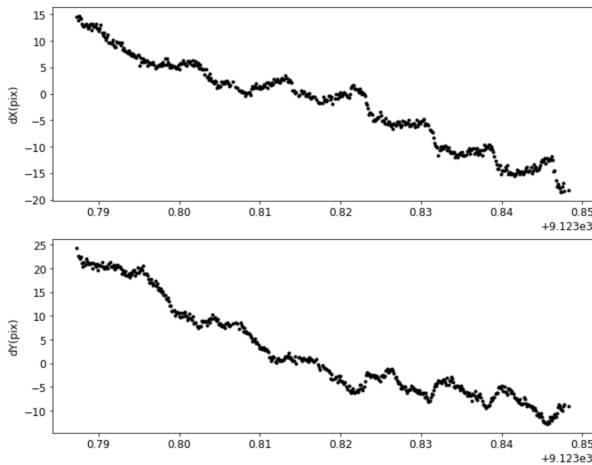
Partially functioning linear stage mechanism in the ip band

Because of a problem with the linear stage mechanism, the photonic diffuser in the ip band cannot be fully inserted into the beam. As a result, the field-of-view is partially obscured by the stage, which appears as a stripe at the east edge of images. (See the figure below.) Observers of bright targets must decide whether a partially obscured image is an acceptable cost for mitigating the likelihood of a saturated image.



Telescope tracking

During commissioning observations two deficiencies in the telescope have resurfaced. The telescope's pointing drifts during unguided observations, and on short time scales, the pointing can jump by up to 2 arcseconds. Because shutter opening times are not synchronized with the tracking cycle, any exposure can be affected by the jumps, although longer exposures are more likely to span a jump than shorter exposures.



Reference star x/y positions during an open-loop tracked planet transit observation. Note the cyclic, sudden jumps in the telescope position.

To preserve image quality, MuSCAT3 observations should be guided. With the decommissioning of the Spectral camera, the 4AG autoguider unit was removed from the telescope. In its place, an inventoried facility guider was installed and restored to service, and a Muscat self-guided mode was introduced. Test observations demonstrated that the tracking errors were successfully suppressed when the facility guider was active.

Field rotation

The (de)rotator on the 2m telescope has an azimuth range slightly greater than one full rotation. For most sky positions, only one derotator position is possible. Consequently, long-duration observations, such as the monitoring of an exoplanet transit, may be terminated when the derotator hits a limit. The derotator limits of the 2m telescope are described in Appendix D of the [“Getting Started” guide](#). We recommend that long-duration observations be broken down into sub-observations, so that the derotator can “unwrap”.

Users should be aware, however, that breaking a request into multiple sub-requests can detrimentally affect the accuracy of photometry since the position of the target on the detector is likely to shift between sub-requests.

Zone of avoidance near Zenith

LCO's 2-meter telescopes have Alt-Az mounts, and the Alt axes are not designed to point the telescopes beyond Alt = 90°, i.e. the zenith. To track an object that passes through the zenith, the Az axis would have to turn the telescope at infinite speed at the moment Alt = 90°. Hence, Alt/Az telescopes usually have a “Zone of Avoidance” around the zenith at which they cannot track an object. On LCO's 2-meter telescopes, tracking performance worsens for zenith distances < 2°. LCO's scheduler does not prevent observations of targets that pass within 2° of the zenith, but **users are advised to avoid long observations of such targets**.

Acknowledgement of MuSCAT3

All papers based on MUSCAT3 data shall contain the following acknowledgement:

“This paper is based on observations made with the MuSCAT3 instrument, developed by the Astrobiology Center and under financial supports by JSPS KAKENHI (JP18H05439) and JST PRESTO (JPMJPR1775), at Faulkes Telescope North on Maui, HI, operated by the Las Cumbres Observatory.”

Relevant links

- [Overview of the MuSCAT3 instrument](#) (updated 4 Nov 2020)
- [Getting Started with MUSCAT API & Portal Requests](#)
- List of [Commissioning and Science Validation Data](#)

Transition-to-operations Timeline

Pre-installation assembly begins: 14 Sep 2020

Installation on Faulkes Telescope North: 27 Sep 2020

First light; engineering commissioning begins: 28 Sep 2020

First science observation: 1 Oct 2020

Observations for science validation projects begin: 8 Oct 2020

Release for routine science observations: 4 Nov 2020

Acknowledgements:

- Photometry comparisons are made to “The ATLAS All-Sky Stellar Reference Catalog”
Tonry, J.L., Denneau, L., Flewelling, H., et al. 2018, ApJ, 867, 105.
doi:10.3847/1538-4357/aae386